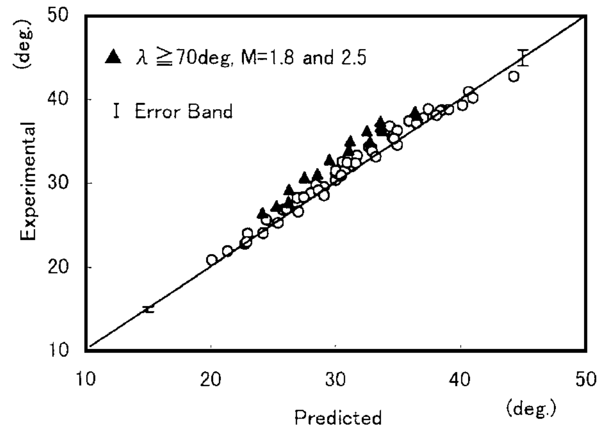

Fig. 2 Comparison of the predicted and experimentally obtained shock angles.

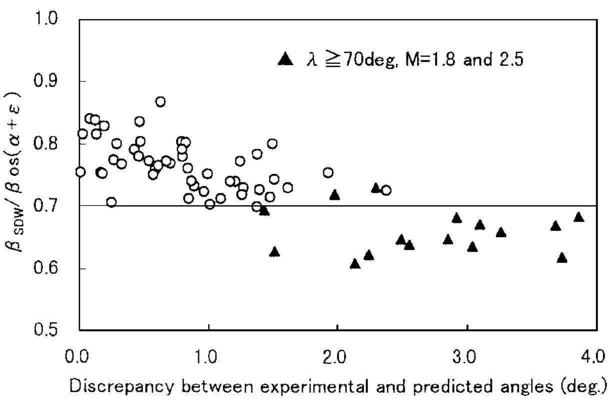

Fig. 3 Shock-curvature effect on discrepancy between experimental and predicted angles.

the prediction improves when the shock becomes flatter at the higher Mach number of 3.5. This shock-curvature effect can be evaluated by a simple nondimensional shock angle, $\beta_{SDW}/\beta_{OS}(\alpha+\varepsilon)$, which indicates a deviation of the SDW shock wave from the planar two-dimensional shock. Figure 3 plots discrepancies between experimental and predicted angles against the nondimensional shock angles. Most of the triangle points fall where $\beta_{SDW}/\beta_{OS}(\alpha+\varepsilon)$ is less than 0.7. If all of the cases less than 0.7 are excluded, then most of the predictions fall within the experimental accuracy shown by the bars in Fig. 2.

Conclusion

It can be concluded that the proposed method is practically accurate enough as long as $\beta_{SDW}/\beta_{OS}(\alpha+\varepsilon)$ is above 0.7. Finally, this procedure can be applied regardless of whether the shock is attached at the leading edge (Fig. 1 shows the attached case only); however, the procedure is not applicable for the cases in which any of α, ε, and $\alpha+\varepsilon$ is above the theoretical attachment limit for the two-dimensional oblique shock at a certain M because β_{OS} is not obtainable for Eq. (5) under such a condition.

References

[1]Koide, S., Saida, N., and Ogata, R., "Correlation of Separation Angles Induced by Glancing Interactions," *AIAA Journal*, Vol. 34, No. 10, 1996, pp. 2198–2200.

[2]Koide, S., Griesel, C. J. W., and Stollery, J. L., "Correlation of Shock Angles Caused by Rhombic Delta Wings," *AIAA Journal*, Vol. 34, No. 7, 1996, pp. 1529–1531.

[3]Koide, S., "Correlation of Shock Angles Caused by Flat Delta Wings," *AIAA Journal*, Vol. 34, No. 9, 1996, pp. 1956–1958.

M. Samimy
Associate Editor

Observations of Supersonic Flat Plate Wake Transition

N. T. Clemens* and M. F. Smith†
University of Texas at Austin, Austin, Texas 78712-1085

I. Introduction

ALTHOUGH the instability and transition of supersonic slender body wakes have seen extensive study for decades, little is known of the topology of the developing vortical structures. Kendall studied the stability of Mach 2–4 flat plate wakes and found that in a quiet wind tunnel, where all wall boundary layers remained laminar, the wake underwent aperiodic transition, i.e., without an identifiable vortex street. In contrast, in a noisy tunnel, where the wall boundary layers were turbulent, a periodic vortex street was observed. In a more recent study, Chen et al.[1] studied three-dimensional time-developing supersonic planar wakes using direct numerical simulation and observed the development of large-scale, three-dimensional structures that are similar to those previously observed in incompressible flat plate wakes.[2]

In this Note, we discuss the results of a primarily flow visualization investigation of the development of instabilities in the near-field region of a Mach 3 flat plate wake. Additional experimental details and results can be found in Ref. 3.

II. Experimental Apparatus and Run Conditions

The experiments were conducted in a pressure-vacuum wind tunnel with a freestream Mach number of 3.0. The test section had a 51×51 mm cross section and a length of 310 mm. The wake was formed using a splitter plate (3-deg full angle and 0.7-mm tip thickness) that began upstream of the nozzle throat and extended 50 mm into the test section. The primary diagnostic method used was planar laser scattering (PLS) from a seeded alcohol fog. The fog was illuminated with a light sheet from a frequency-doubled Nd:YAG laser, and the images were acquired using a charge-coupled device video camera.

Results are presented for stagnation and test section static pressures of 80 ± 4 kPa and 2 ± 0.02 kPa absolute, respectively, a stagnation temperature of 290 ± 3 K, a freestream Mach number of 3.0, and a Reynolds number based on plate length from the throat of $Re_L = 1.4 \times 10^6$. The splitter plate boundary layers were laminar and were measured with a pitot tube (with a sharp flattened tip, 0.3 mm high $\times$ 1 mm wide) to have a thickness of $\delta_{99} = 1.9 \pm 0.1$ mm. The side wall boundary layers were transitional, probably owing to being tripped by test section/nozzle and test section/window junctions.

III. Results

Mean pitot pressure profiles across the wake were obtained at several downstream locations. The pitot pressure measurements were converted to velocity profiles using the Rayleigh pitot formula and the assumption of adiabatic flow. The wake momentum thickness was computed from these profiles to be $\theta = 0.3 \pm 0.02$ mm at all stations. As a means of quantifying the level of compressibility in the wake, the relative Mach number defined as $M_r = (U_\infty - U_c)/a_\infty$ is used, where U_∞ is the freestream velocity, U_c is the wake centerline velocity, and a_∞ is the freestream sound speed. The relative Mach number variation as a function of downstream position is shown in Fig. 1. The coordinate system is defined to have the x, y, and z coordinates as representing the streamwise, cross-stream, and

Presented as Paper 96-0785 at the AIAA 34th Aerospace Sciences Meeting, Reno, NV, Jan. 15–18, 1996; received Sept. 20, 1997; revision received March 17, 1998; accepted for publication March 18, 1998.

*Assistant Professor, Department of Aerospace Engineering and Engineering Mechanics. Senior Member AIAA.

†Graduate Student, Department of Aerospace Engineering and Engineering Mechanics.

spanwise directions, respectively, with the origin corresponding to the splitter plate tip.

Sample side-view (x–y plane) PLS images are shown in Fig. 2, which is composed of three images that are uncorrelated in time, and the flow is from left to right. The gray-scale images render high scattering levels as light and low scattering as dark. The freestream is light due to the presence of the fog, whereas low-velocity (hence high-temperature) regions are dark due to droplet evaporation. In regions that are not so warm as to evaporate the fog, the scattering signal is proportional to the fluid density. We caution that, because the images of Fig. 2 were taken at different times, it is possible that the sequence of three images does not represent the actual evolution of wake structures; however, other images taken with twice as large a field of view show that the development of the structures seen in the upstream two images of Fig. 2 is quite common.

In Fig. 2 the initially laminar wake is seen as the dark stripe at the far left that extends to about $x/\theta = 15$. Below the laminar wake is a dark region that is an artifact caused by a reflection from the splitter plate. The laminar wake is typically seen to form a vortex street, although we note that it can also transition without an identifiable street (although this is substantially less common). This observation is in apparent agreement with Kendall because in the present study the side wall boundary layers were transitional; thus, both periodic and aperiodic transition may be expected. It is notable how similar the vortex structure is to that of incompressible flat plate wakes, particularly considering the high relative Mach number in the near field.

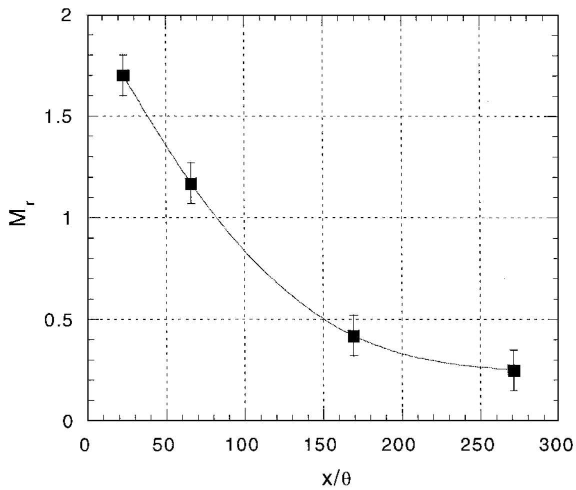

Fig. 1 Variation of the relative Mach number with downstream distance.

Despite the similarities to incompressible wakes, there are also indications of compressibility effects. The most obvious are the weak eddy shocklets that can be seen by careful inspection of the first image (particularly on the lower side of the wake at the horizontal center of the image). Eddy shocklets were observed over the approximate range of $x/\theta < 90$, corresponding approximately to $M_r > 0.9$. Similar eddy-induced shocks have been observed in base flows and shear layers[4,5] and in simulations of supersonic shear layers.[6]

Because the scattering signal outside of the vortices is proportional to fluid density, we can see that there exists a broad expansion fan originating just downstream of the vortex cores, downstream of which the flow recompresses via an eddy shocklet or, in some cases, apparently through a continuous compression wave. The shocklets are typically curved as they exhibit a steeper angle closer to the wake and then coalesce with the weak expansion wave emanating from the splitter tip. This general description of the shocklets is similar to that proposed by Dimotakis[7] for compressible turbulent shear layers. The density ratio across the upper row of shocklets can be as high as 1.3, indicating that the normal component of the upstream Mach number is about 1.18, suggesting the shocklets, although weak, are stronger than Mach waves.

Sample plan-view PLS images are shown in Fig. 3, where the laser sheet cuts through the centerline of the wake, i.e., at $y = 0$. The width of the field of view is 19 mm; thus the side walls are about 15 mm from the top and bottom edges of the images. The first half of the first panel is completely dark because the laser sheet cuts through the laminar wake. Light regions first appear where the wake has rolled up into vortices that entrain freestream fluid. In the upstream images, the alternating dark and light bands suggest the vortices are approximately two dimensional. The vortices rapidly become distorted on a large scale, as seen by the tilting in Fig. 3, and the nearly periodic convolution observed in other images.[3] In addition, small-scale instabilities rapidly develop as seen in Fig. 3, where the influence of a nearly periodic sequence of vortices can be seen on the downstream edge of the first two white bands. These vortices are most likely related to the vortices identified in the strained braid regions in incompressible wakes.[2] By the third station, flow structure can remain quasi-two-dimensional as in Fig. 3 or it can appear as three-dimensional turbulence.[3]

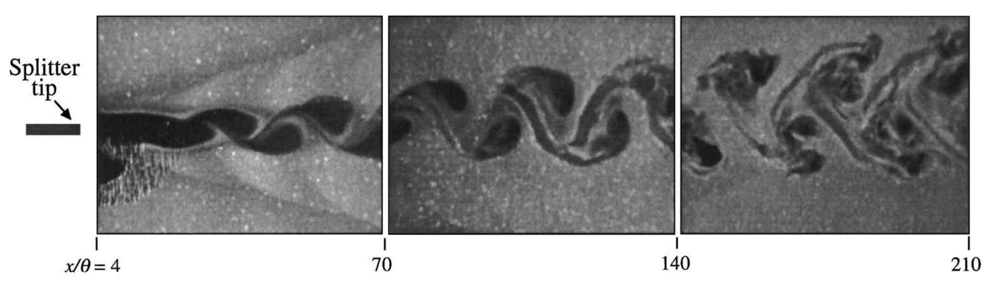

Fig. 2 Uncorrelated side-view PLS images taken at three different downstream locations.

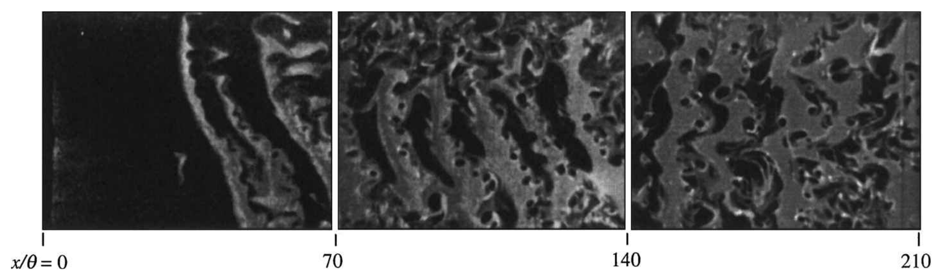

Fig. 3 Uncorrelated plan-view PLS images (laser sheet cuts through the wake centerline).

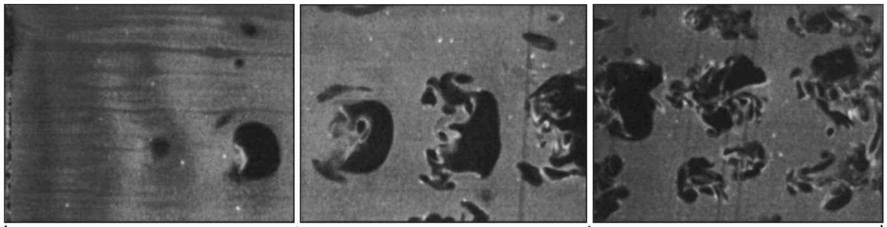

Fig. 4 Uncorrelated plan-view PLS images. (Laser sheet is tilted at a 3-deg angle.)

At the top of the middle image, there is a region that is highly three dimensional. This is believed to be due to contamination from turbulence that originated from the outer regions of the upstream splitter plate boundary layers. We believe that the outboard regions of the splitter plate boundary layers were forced to undergo transition by the unsteady plate/side wall corner vortices.

Plan-view PLS images are shown in Fig. 4 where the laser sheet was rotated about the z axis by about 3 deg, thus allowing the visualization of the outer part of the wake. The upstream half of the leftmost image reveals primarily two-dimensional light and dark bands. In this region the laser sheet does not pass through the laminar wake but just outside of it. The initial spanwise bands at left distort with downstream distance, after which dark round islands of wake fluid appear. The dark islands apparently result from the bending and uplifting of the spanwise vortices. The second image downstream shows that the spanwise vortices become highly three dimensional and sometimes form a horseshoe-shaped structure. The horseshoe-shaped structures are similar to those seen in incompressible flat plate wakes[2] and in numerical simulations of compressible planar wakes.[1]

IV. Conclusions

A preliminary experimental study has been conducted of the laminar-to-turbulent transition of a Mach 3 flat plate wake. Side-view PLS images reveal a vortex street that is remarkably similar to that found under incompressible conditions. Plan-view images show that the initially two-dimensional vortex street rapidly develops both small- and large-scale, three-dimensional instabilities. The effect of the large-scale instability is to cause the spanwise vortices to distort into horseshoe-shaped structures. Furthermore, unlike incompressible wakes, the side-view images reveal that the vortices generate weak eddy shocklets for supersonic relative Mach numbers.

Acknowledgment

We would like to thank James Kendall (Jet Propulsion Laboratory) for providing us with a detailed description of some of his unpublished work on flat plate supersonic wakes.

References

[1]Chen, J. H., Cantwell, B. J., and Mansour, N. N., "The Effect of Mach Number on the Stability of a Plane Supersonic Wake," *Physics of Fluids A*, Vol. 2, No. 6, 1990, pp. 984–1004.

[2]Meiburg, E., and Lasheras, J., "Experimental and Numerical Investigation of the Three-Dimensional Transition in Plane Wakes," *Journal of Fluid Mechanics*, Vol. 190, 1988, pp. 1–37.

[3]Clemens, N. T., Smith, M. F., and Fernandez, J. V., "Observations of Supersonic Flat Plate Wake Transition," AIAA Paper 96-0785, Jan. 1996.

[4]Smith, K. M., and Dutton, J. C., "Large-Scale Structures in Supersonic Reattaching Shear Flows," AIAA Paper 95-2251, June 1995.

[5]Alvi, F. S., Krothapalli, A., and Washington, D., "Fluctuating Pressure Measurements in a Highly Compressible Countercurrent Turbulent Shear Layer," AIAA Paper 95-2175, Jan. 1995.

[6]Vreman, B., Kuerten, H., and Geurts, B., "Shocks in DNS of the Three-Dimensional Mixing Layer," Proceedings of the Tenth Symposium on Turbulent Shear Flows, Pennsylvania State Univ., 1995.

[7]Dimotakis, P. E., "Turbulent Free Shear Layer Mixing and Combustion," *High-Speed Flight Propulsion Systems*, edited by S. N. B. Murthy and E. T. Curran, Vol. 137, Progress in Astronautics and Aeronautics, AIAA, Washington, DC, 1991, pp. 265–340.

W. Oberkampf
Associate Editor

Interaction of Large Three-Dimensional Eddies and Small Streamwise Vortices

Roy Y. Myose*
Wichita State University, Wichita, Kansas 67260-0044
and
Ron F. Blackwelder†
University of Southern California, Los Angeles, California 90089-1191

Introduction

PAST studies have shown that at least two types of organized structures exist in turbulent boundary layers.[1,2] In the outer region are large-scale motions on the size of the boundary-layer thickness δ. Near the wall are small-scale, low- (and high-) speed streamwise streaks, and viscous ($^+$) scaling with the kinematic viscosity ν and friction velocity u_τ is used for these small-scale structures. In a sequence of events called the bursting process, the low-speed streaks lift up off the wall, oscillate, and then break down.[3] This bursting process is responsible for most of the turbulent energy production near the wall.[4] The evolution and breakdown of streamwise vortices are thought to be closely associated with the structure and breakdown of the bursting process.[5,6] In the outer region, the large-scale motion consists of $-\omega_z$ spanwise vortical motion, which entrains nonturbulent fluid from outside the boundary layer.[7,8] At the upstream interface between turbulent and nonturbulent regions, there is an outward movement of fluid away from the wall ahead of the interface and an insweep of high-speed fluid toward the wall behind the interface.[8,9]

In flow visualization studies,[10–12] the bursting process was often followed by an insweep of high-speed fluid. This suggests an interactive relationship between near-wall and outer-region structures. However, both structures appear randomly in space and time, which makes it difficult to study their exact interactive relationship. To address this issue, Myose and Blackwelder[13] devised an experiment to emulate these structures with the proper size and strength but in a deterministic and periodic manner. Reference 13 used Görtler streamwise vortices to emulate the near-wall structure and large two-dimensional spanwise vortices shed from a pitch oscillating airfoil to emulate the outer-region structure. The near-wall vortices initially became unstable due to the normal and spanwise inflectional velocity profiles associated with the wall vortices. Breakdown of the wall vortices was subsequently triggered by the arrival of high-speed fluid associated with the outer region. Increasing the large spanwise vor-

Presented as Paper 97-0442 at the AIAA 35th Aerospace Sciences Meeting, Reno, NV, Jan. 6–9, 1997; received June 20, 1997; revision received February 18, 1998; accepted for publication March 9, 1998.

*Associate Professor, Department of Aerospace Engineering. Associate Fellow AIAA.

†Professor, Department of Aerospace Engineering. Associate Fellow AIAA.